



Tunable luminescence properties and energy transfer behaviour in Bismuth sensitized $\text{LaInO}_3:\text{Tb}^{3+}$ phosphors

K. Sujatha¹, T.K.Visweswara Rao², Ch. SatyaKamal³, K.Samatha⁴,
Y.Ramakrishna⁵, K.RamachandraRao^{6*}

- ^{1,2,3,6}Crystal Growth and Nano-Science Research Center, Department of Physics, Government College (A), Rajamahendravaram, Andhra Pradesh, India-533105
^{3,6}Department of Physics, Adikavi Nannaya University, Rajamahendravaram, Andhra Pradesh, India
⁴Department of Physics, Andhra University, Visakhapatnam, Andhra Pradesh-India-530003
⁵Department of Engg., Physics, Andhra University, Visakhapatnam, Andhra Pradesh-India-530003

Abstract : A series of $\text{Bi}^{3+}:\text{Tb}^{3+}$ doped LaInO_3 phosphors were synthesized via Polyol method. The structure and luminescence properties were investigated. The optimum concentrations of Bi^{3+} and Tb^{3+} were 3mol% and 3mol%, respectively. Furthermore, $\text{LaInO}_3:3\text{Bi}^{3+}$ and $\text{LaInO}_3:3\text{at}\%\text{Tb}^{3+}$ phosphors emitted blue and green light and the emission color of $\text{LaInO}_3:\text{Bi}^{3+}$, Tb^{3+} could be tuned from blue to green through the energy transfer. This energy transfer from Bi^{3+} to Tb^{3+} was confirmed and investigated by photoluminescence spectrum and decay lifetime. With constantly increasing Tb^{3+} concentrations, the energy transfer efficiency from Bi^{3+} to Tb^{3+} in LaInO_3 host increased gradually and reached as high as 64%. The energy transfer mechanism ($\text{Bi}^{3+}-\text{Tb}^{3+}$) was proved to be dipole-dipole mechanism. Moreover, the phosphor of $\text{LaInO}_3:3\text{at}\%\text{Bi}^{3+}$, $3\text{at}\%\text{Tb}^{3+}$ could exhibit strong green emission with good CIE chromaticity coordinate. The results indicate that $\text{LaInO}_3:3\text{at}\%\text{Bi}^{3+}$, $3\text{at}\%\text{Tb}^{3+}$ is a potential green emitting phosphor for the application in LED and display field.

Keywords : Bi^{3+} Co-doping, $\text{LaInO}_3:\text{Tb}^{3+}$, Photoluminescence, Spectral overlap, Energy Transfer.

1. Introduction

Recently development of phosphor materials for field emission display (FED) technology is highly focused due to several interesting properties when compared to the traditional cathode ray tube (CRT) phosphors, such as high electric conductivity, low surface recombination velocities, vacuum compatibility, hazardlessness to cathodes, and the ability to withstand high current densities[1]. However, highly efficient phosphors are desired for FEDs to have decrement in energy consumption, higher resistance to current saturation, and higher chemical stability. Many reports [2–4] indicate that oxide based phosphors, which are semiconductor have shown remarkable field emission properties. Among many semiconductor based oxide phosphors, Lanthanum Indium oxide (LaInO_3) with a bandgap of 3.2 eV have been found to be the promising candidate, with sufficient conductivity to overcome the charge build-up on the phosphor surfaces[5,6]. Rare-earth doped LaInO_3 phosphors have been reported as an alternative luminescence material

due to their high thermal and chemical stabilities. Silicon coated core-shell structured $\text{LaInO}_3: \text{Sm}^{3+}, \text{Tb}^{3+}$ phosphors have been used for their diverse luminescent properties[7-9].LI.vanSteenselet.al showed that $\text{LaInO}_3: \text{Bi}^{3+}$ is an efficient, blue-emitting phosphor material[10].

It is well-known that the Tb^{3+} ion is a most important green light emitting luminescent activator, the $^5\text{D}_4-^7\text{F}_5$ transition peaking around 543 nm leads to the predominantly green emission. Nevertheless, due to the f-f forbidden transition, the intensities of Tb^{3+} absorption peaks in the NUV region are quite weak and the width is very narrow so a sensitizer ion which strongly absorbs excitation energy in the NUV region is necessary [11-13]. In order to enhance Tb^{3+} absorption in the NUV region, one of the most feasible way is to introduce (such as $\text{Ce}^{3+}, \text{Eu}^{2+}, \text{Sb}^{3+}$ and Bi^{3+}) sensitizer to transfer energy to Tb^{3+} effectively. The Bi^{3+} can serve as sensitizer in phosphors with their large cross-section to capture excitation energy efficiently and then transfer it to the activator ions (Tb^{3+} ions)[14-17]. Moreover emission spectrum of Bi^{3+} ion varies from blue to green region for different host lattices[18] because outer $6s^2$ electronic configurations of Bi^{3+} depend strongly on their environmental conditions, such as covalence, coordination number and site symmetry[19-22].

In this study, $\text{Bi}^{3+}, \text{Tb}^{3+}$ co-doped LaInO_3 phosphors have been prepared by polyol method, and their structural, morphological, luminescence properties, decay lifetime, energy transfer, color chromaticity have been systematically studied. $\text{Bi}^{3+}, \text{Tb}^{3+}$ co-doped LaInO_3 phosphors can be effectively excited by NUV (Near Ultra-Violet) light and emit visible light from blue to green by changing the concentrations ratio of Bi^{3+} . The results show that it may have potential applications in white light-emitting phosphor for display applications.

2. Experimental details

2.1 Preparation of the particles

For preparation of pure and doped LaInO_3 samples, $\text{La}(\text{NO}_3)_3 \cdot 6\text{H}_2\text{O}$ [Sigma-Aldrich 99.9%], $\text{In}(\text{NO}_3)_3 \cdot \text{H}_2\text{O}$ [Alfa Aesar 99.99%], $\text{Bi}(\text{NO}_3)_3 \cdot 5\text{H}_2\text{O}$ [Sigma-Aldrich 99.9%], $\text{Tb}(\text{NO}_3)_3 \cdot 6\text{H}_2\text{O}$ [Sigma-Aldrich 99.9%] were used as starting materials without any further purification. Polyol route was adopted for synthesis; ethylene glycol serves as the solvent and urea for hydrolysis. For preparing the undoped lanthanum indate (LaInO_3), initially stoichiometric amounts of $\text{La}(\text{NO}_3)_3 \cdot 6\text{H}_2\text{O}$ and $\text{In}(\text{NO}_3)_3 \cdot \text{H}_2\text{O}$ was transferred into a two-necked RB flask containing solution of 20ml ethylene glycol. The solution was kept under magnetic stirring and continuous heating. When the temperature was at 100°C , around 2 gram urea was added and temperature was raised further to 120°C and kept up at this temperature for 2 hours. The formed precipitate was cooled, centrifuged, washed thrice with methanol, twice with acetone and allowed to dry overnight at room temperature. Then the samples were sintered in a muffle furnace at a temperature of 1000°C for 5h. Finally, the samples are naturally cooled down to room temperature and fully ground for further investigations. The above procedure was repeated for the preparation of Bi and Bi-Tb LaInO_3 samples by dissolving required amount of $\text{Bi}(\text{NO}_3)_3 \cdot 5\text{H}_2\text{O}$ $\text{Tb}(\text{NO}_3)_3 \cdot 6\text{H}_2\text{O}$ in ethylene glycol.

2.2 Characterization Techniques

X-ray diffraction (XRD) studies were carried out using a Philips powder X-ray diffractometer (model PW 1071) with Ni filtered $\text{Cu-K}\alpha$ radiation. For calibration purpose, diffraction peak corresponding to the (111) plane of Si at a 2θ value of 28.442° was employed. The lattice parameters were obtained from the XRD patterns using POWDERX software. SEM instrument used was from Seron Inc. (Model AIS 2100) having standard tungsten filament. An accelerating voltage of 20 kV and magnification of 10 kx was used for recording the micrographs. All luminescence measurements were carried out at room temperature with a resolution of 5 nm, using Edinburgh Instruments FLSP 920 system attached with a 450 W Xe lamp as the excitation source. A micro second flash lamp and a nanosecond hydrogen flash lamp was used for lifetime measurements.

3. Results & Discussion

3.1 Phase identification, Structure and Morphology

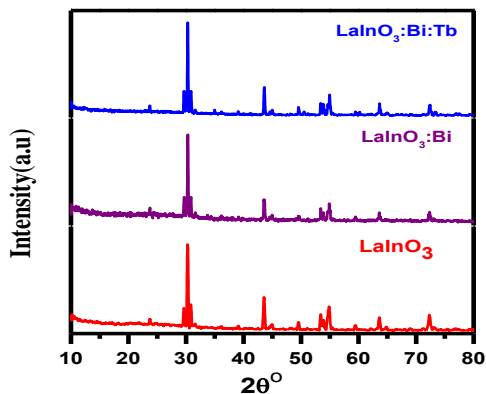


Fig 1. XRD patterns corresponding to pure LaInO₃, Bi³⁺ doped LaInO₃, LaInO₃: 3 at.% Bi³⁺, 3at.% Tb³⁺ at 1000 °C

Fig. 1 shows the diffraction patterns of the undoped and LaInO₃: 3 at.% Bi³⁺, LaInO₃: 3 at.% Bi³⁺, 3 at.% Tb³⁺ nanophosphors sintered at 1000 °C. All X-ray diffraction patterns are indexed to pure orthorhombic phase (JCPDS No. 08–0148) with *Pnma* space group and there are no formations of impurity phases. In general the crystallite size is estimated from the Scherrer’s equation, $D_{hkl} = 0.9\lambda/\beta\cos\theta$, where *D* is the average crystallite size, λ is the X-ray wavelength (1.5406 Å), θ is the diffraction angle and β is the full-widths at half-maximum (FWHM) of observed peak (30.29°). The strongest diffraction peaks are used to calculate the crystallite size of the samples. The calculated average crystallite size is 100 nm. The lattice parameters of the synthesized nanophosphors calculated by least square fitting using POWDERX software are illustrated in Table 1.

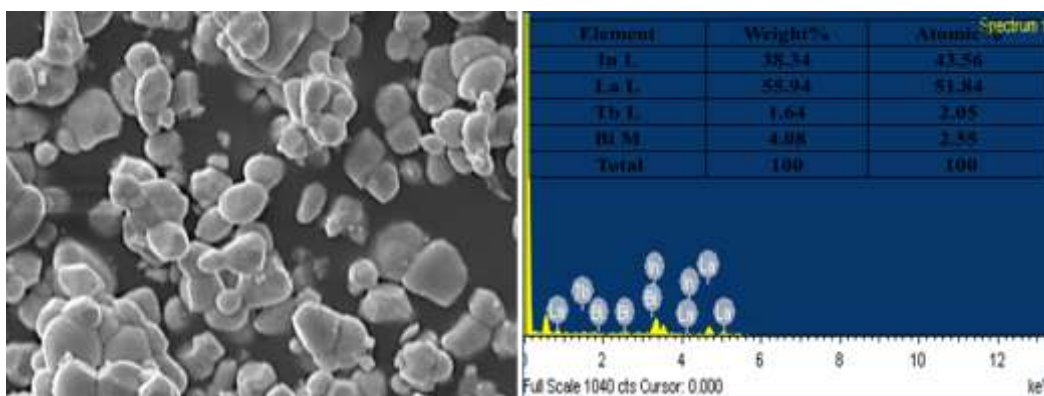


Fig. 2. SEM images and EDAX spectra’s of Bi³⁺, Tb³⁺ doped LaInO₃

Table.1 Unit cell parameters of LaInO₃, LaInO₃:Bi³⁺:Tb³⁺

Composition	a(Å)	b(Å)	c(Å)
LaInO ₃	5.782	8.336	5.999
LaInO ₃ :Bi ³⁺	5.775	8.245	5.928
LaInO ₃ : Bi ³⁺ , Tb ³⁺	5.745	8.016	5.799

Fig. 2 shows the morphology and chemical composition of $\text{LaInO}_3: 3 \text{ at.}\% \text{ Bi}^{3+}, 3 \text{ at.}\% \text{ Tb}^{3+}$ nanophosphors. The LIO (Lanthanum Indium oxide) powder particles are in nanometerrange and nearly all of the particles are spherical morphology, which agglomerate to larger material. The average particle size is between 100 and 200 nm. It is well known that, particles with spherical shaped ($<2 \mu\text{m}$) are of great importance because of their high packing density, lower scattering of light, brighter luminescent performance, high definition and more improved screen packing density [23]. Energy dispersive X-ray spectrometry (EDS) analysis was used to determine the composition of the samples and it shows good agreement with the nominal sample composition.

3.2 Photoluminescence and Lifetime measurements

1, 3 and 5 % bismuth doped LaInO_3 samples were heated at 1000°C and also investigated for their emission, excitation and decay spectra. All samples have broad emission band centered at 432 nm which is attributed to ${}^3\text{P}_1 - {}^1\text{S}_0$ transition of Bi^{3+} ions on excitation with 330 nm [24] and observed the intensity of the 432 nm emission band with increasing Bi^{3+} concentration and reaches a maximum at 3 at.%, and then afterwards emission intensity decreases due to concentration quenching effect. The respective steady state, decay graphs and life time values were reported by our group previously[25].

Fig. 3 represents excitation spectra of $\text{LaInO}_3:\text{Tb}^{3+}(3 \text{ at.}\%)$ (λ_{em} monitored at 543 nm) and emission spectra of (excited with 330 nm) $\text{LaInO}_3:\text{Bi}^{3+}(3 \text{ at.}\%)$ samples. The considerable spectral overlap of an emission band and the excitation band indicates an effective radiative energy transfer (ET) is possible. Therefore, it was expected that an efficient energy transfer can occur from Bi^{3+} to Tb^{3+} . Apart from the spectral overlap, the evidence for the energy transfer occurring between Bi^{3+} to Tb^{3+} is been explained in the flowing section.

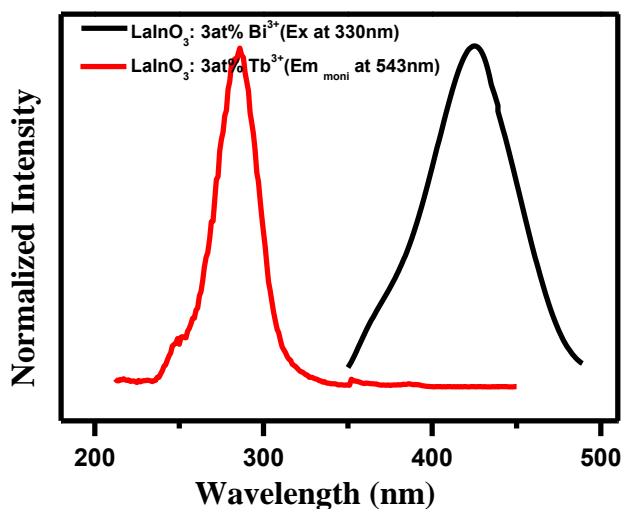


Fig. 3 Spectral overlap of excitation spectra of $\text{LaInO}_3: \text{Tb}^{3+}(3\text{at}\%)$ and emission spectra of $\text{LaInO}_3:\text{Bi}^{3+}(3 \text{ at.}\%)$ samples heated up to 1000°C

In order to further study the ET from Bi^{3+} to Tb^{3+} , a series of $\text{LaInO}_3: 3 \text{ at.}\% \text{ Bi}^{3+}, 1, 3, 5 \text{ at.}\% \text{ Tb}^{3+}$ samples have been prepared. The PL emission spectra of samples sintered at 1000°C , excitation with 330 nm were presented in Fig. 4(a). On increasing of Tb^{3+} ions concentrations, the Tb^{3+} emission intensity persistently increases until the Tb^{3+} concentration is above 0.03, and then decreases because of concentration quenching effect, while the intensity of the Bi^{3+} emission decreases although the content of Bi^{3+} was fixed. As shown in Fig. 4(a), the emission intensity bands of Tb^{3+} were obviously enhanced as Bi^{3+} incorporated. The above variations in the emission intensities of the Bi^{3+} and Tb^{3+} ions strongly proved the occurrence of the ET from Bi^{3+} to Tb^{3+} ions. The excitation spectra (Fig. 4(b)) of $\text{LaInO}_3: \text{Bi}$ and Tb co-doped samples were wider than 3at% Tb doped LaInO_3 sample indicated that the absorption band of $\text{LaInO}_3: 3 \text{ at.}\% \text{ Bi}^{3+}, 1, 3, 5 \text{ at.}\% \text{ Tb}^{3+}$ samples consist of a Bi^{3+} excitation band, which can predict that Bi^{3+} can transfer energy to Tb^{3+} in LaInO_3 host. The relative emission intensities of Tb^{3+} ions at 543 nm and Bi^{3+} ions at 432 nm as a function of Tb^{3+} concentration

were shown in Fig. 5(a).In order to further verify the effect of Bi³⁺ doping in enhancing the PL intensity, single doped Tb³⁺: LaInO₃ emission spectra are shown in Fig.5(b).

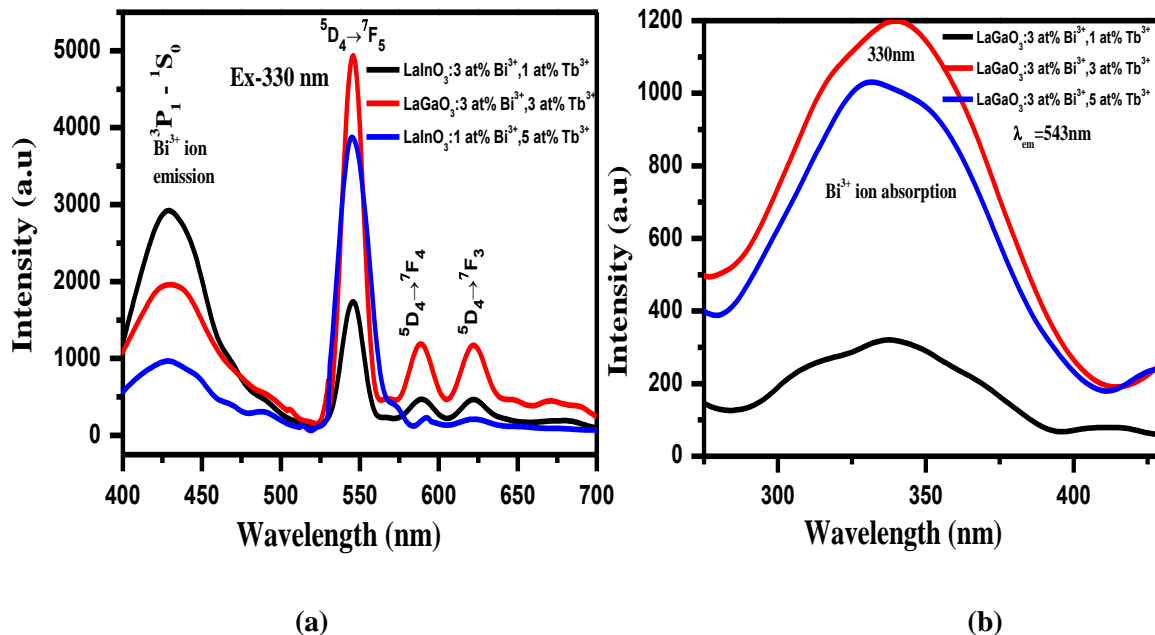


Fig. 4. Plots representing intensity of the (a) emission and (b) excitation spectra of LaInO₃: 3 at.% Bi³⁺ (1, 3, 5 at.%) Tb³⁺.

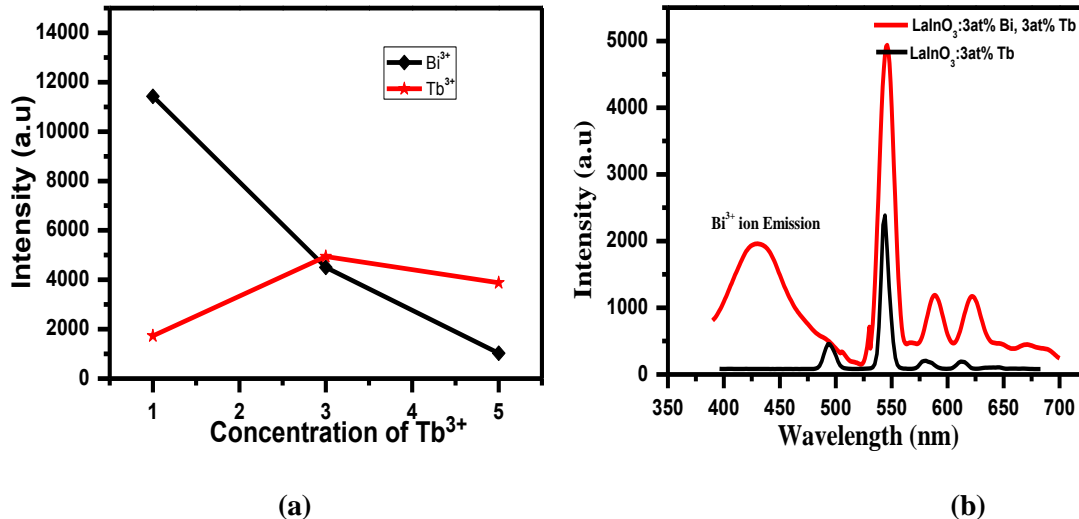


Fig. 5.(a) Intensity variation of Bi³⁺ as a function of Tb³⁺ ions (b) Comparison of single doped (a) Tb³⁺ (Ex at 286 nm and monitored at 543 nm) and LaInO₃ Bi³⁺: Tb³⁺ co-doping heated up to 1000 °C.

In order to certify and investigate the ET from Bi³⁺ to Tb³⁺ further, the decay curves of Bi³⁺ and Tb³⁺ emission of LaInO₃: 3 at.% Bi³⁺, 1, 3, 5 at.% Tb³⁺ phosphors have been measured and shown in Fig. 6(a) and (b) respectively. The decay curves were well fitted with a double-exponential rule according to the following equation:

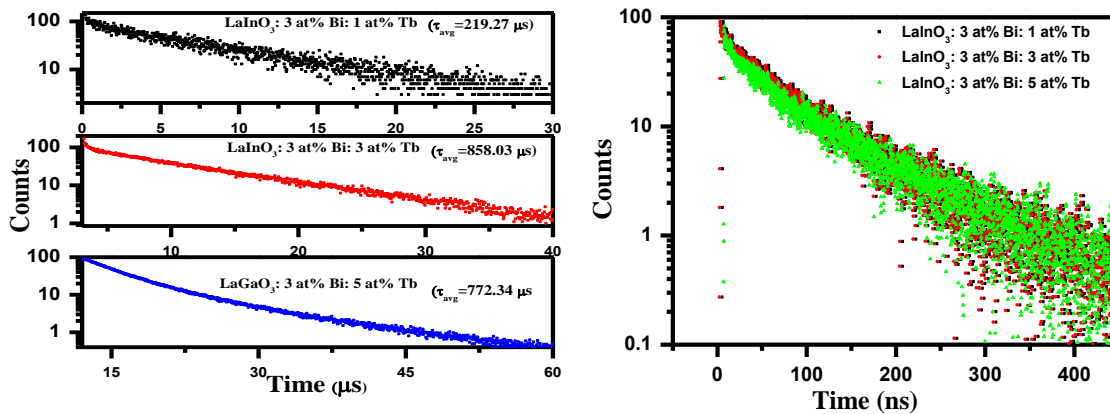
$$I = A_1 \exp\left(\frac{-t}{\tau_1}\right) + A_2 \exp\left(\frac{-t}{\tau_2}\right) \quad (1)$$

where I is the luminescence intensity at the time t , τ_1 and τ_2 are two components of the decay time, A_1 and A_2 are constants.

According to these parameters, the average decay times of LaInO₃: 3 at.% Bi³⁺, 1, 3, 5 at.% Tb³⁺ can be calculated according to the following formula:

$$\tau = \frac{A_1\tau_1^2 + A_2\tau_2^2}{A_1\tau_1 + A_2\tau_2} \quad (2)$$

with increasing the concentrations of doped Tb³⁺, there is a decreased life time of Bi³⁺ (from 181 to 126 ns) Fig.6(b). The decay times of corresponding Tb³⁺ are 219, 858, 772 μs shown in Fig. 6(a). The corresponding energy level diagram of LaInO₃:Bi³⁺, Tb³⁺ with optical transitions and energy transfer process are displayed in Fig.7.



(a) (b)
Fig. 6(a & b). Decay curves of Tb³⁺ and Bi³⁺ in LaInO₃

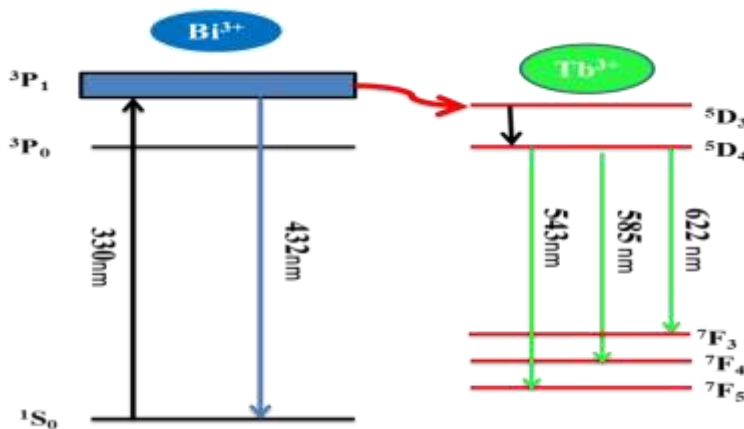


Fig 7. Energy level diagram of LaInO₃: Bi³⁺, Tb³⁺

3.3 Energy Transfer (ET) mechanism

The schematic diagram of ET between Bi³⁺ and Tb³⁺ was presented in Fig. 7. Firstly, the Bi³⁺ ion was excited by the UV light to a high energy level and then relaxes to a lower energy level ³P₁. Partial of the absorption energy has been released in the form of broad-band emission of 432 nm light; the other part was contributed by the energy transfer process from Bi³⁺ to the Tb³⁺. Subsequently, the absorbed energy can be transferred to the ⁵D₃, which relaxed to ⁵D₄ later, or directly to the ⁵D₄ level of Tb³⁺. Finally, the ⁵D₄ level gives the strong emission of Tb³⁺ (⁵D₄-⁷F_J).

The ET efficiency η_{ET} of Bi³⁺ - Tb³⁺ can be calculated using the following equation [26]

$$\eta_{ET} = 1 - \frac{\tau_s}{\tau_{s0}} \quad (3)$$

Where τ_s and τ_{s0} represent the life time values of sensitizer Bi^{3+} in the presence and absence of Tb^{3+} . The energy-transfer efficiency η_{ET} values from Bi^{3+} to Tb^{3+} for LaInO_3 are tabulated in Table 2.

Table 2. ET efficiency of the phosphors

Phosphor	X	$\eta_{\text{ET}}(\%)$
$\text{LaInO}_3: 3\text{at.}\% \text{Bi}^{3+},$ $x \text{Tb}^{3+}$	1	46
	3	55
	5	64

The resonant energy-transfer mechanism from a sensitizer (Bi) to an activator (Tb) in a phosphor consists of two interaction types: exchange and multipolar interaction. If energy transfer takes the exchange interaction, the critical distance between sensitizer and activator should be shorter than 5\AA . When the value reaches the critical transfer distance, the electric multipolar interaction will take place. The critical distance R_c between Bi^{3+} and Tb^{3+} in the LaInO_3 host can be estimated by the following equation [27]:

$$R_c \approx 2 \left(\frac{3V}{4\pi X_c Z} \right)^{1/3} \quad (4)$$

where, V is the volume of the unit cell, X_c is the total critical concentration of dopant ions, while Z represents the number of the activator ions in the unit cell. Using the parameters of LaInO_3 host ($V = 289.63 \text{\AA}^3$, $Z = 2$) and the estimated critical concentration of dopant ions (Bi^{3+} - Tb^{3+}) ($X_c = 0.06$ (As Bi^{3+} optimum is 3% written in decimal form 0.03, similarly for Tb^{3+} optimum is 0.03 adding together $X_c = 0.06$)), the critical distance $R_{\text{Bi-Tb}}$ is calculated to be 16.64\AA , which is much longer than 5\AA , implying that little possibility of ET via the exchange interaction mechanism. Consequently, the transfer between the Bi^{3+} ions and Tb^{3+} ions mainly takes place via electric multipolar interactions.

To further research the ET mechanism from Bi^{3+} to Tb^{3+} ions, it is well-known that the impurities can affect the luminescence properties, but it has the minute influence. Therefore, the interaction type between sensitizers or between sensitizer and activator can be calculated by the following equation [28]:

$$\frac{I}{x} = K[1 + \beta(x)^{\theta/3}]^{-1} \quad (5)$$

where x is the concentration of the activator ions (Bi^{3+} and Tb^{3+} ions), I is the emission intensity, K and β are constants for the same excitation condition for a given host lattice, and θ is a function of multipole-multipole interaction. When the value of θ is 6, 8, or 10, the interaction types correspond to dipole-dipole (d-d), dipole-quadrupole (d-q), and quadrupole-quadrupole (q-q) interactions, respectively. The dependence of $\log(I/x)$ on $\log(x)$ was found to be relatively linear, and it yields a straight line with a slope equal to $\theta/3$, so we can obtain the θ value to study the energy-transfer process between Bi^{3+} and Tb^{3+} in LaInO_3 host. As shown in Fig. 7 the slope of the straight line is $-\theta/3 = -1.70$ based on the PL data of this series of $\text{LaInO}_3:3\text{at}\% \text{Bi}^{3+}$, (1, 3, 5 at %) Tb^{3+} samples. The calculated value of θ is 5.10, which is close to six, meaning that the dipole-dipole interaction is the dominant mechanism for the interaction of Bi^{3+} and Tb^{3+} in the LaInO_3 phosphors.

The color coordinates are shown in Fig. 9. With the increasing of Tb^{3+} concentrations, the chromaticity coordinates systematically change from A to C points which are shown in CIE diagram and point @ is representative of Bi single doped in LaInO_3 phosphor. Corresponding color can be changed gradually from blue to green by adjusting the doping concentrations of Tb^{3+} . The tuned luminous color with codoped Bi^{3+} provides a promising application of Tb^{3+} activated LaInO_3 phosphors in LEDs and FEDs applications.

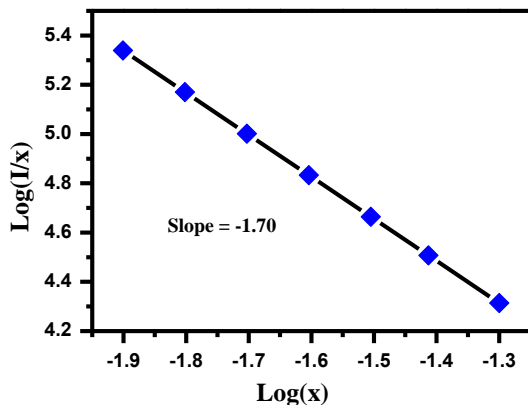


Fig. 8 The fitting line of $\log(I/x)$ vs. $\log(x)$ in $\text{LaInO}_3:3\text{at}\% \text{Bi}^{3+}, 3\text{at}\% \text{Tb}^{3+}$ phosphors beyond the quenching concentration.

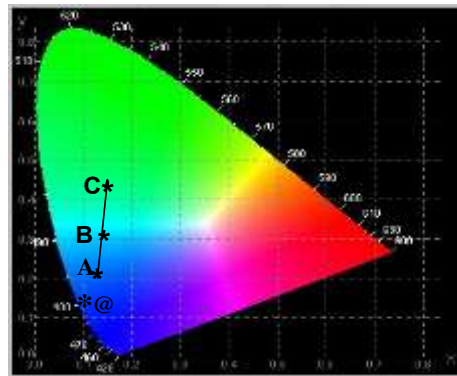


Fig.9 CIE chromaticity diagram

Conclusions

The novel green tunable phosphors, $\text{LaInO}_3: \text{Bi}^{3+}:\text{Tb}^{3+}$ have been synthesized via polyol method and the structure, luminescence properties were investigated. The ET from Bi^{3+} to Tb^{3+} in LaInO_3 host was confirmed. The relative intensity of $\text{LaInO}_3:\text{Tb}^{3+}$ phosphor can be enhanced significantly with the Bi^{3+} co-doping due to ET between Bi^{3+} and Tb^{3+} ions. Furthermore, the phosphor $\text{LaInO}_3:3\text{at}\% \text{Bi}^{3+}, 3\text{at}\% \text{Tb}^{3+}$ exhibited a strong green emission with good CIE chromaticity coordinate. After co-doping $\text{Bi}^{3+}, \text{Tb}^{3+}$, the color rendering, luminous intensity and the absorption intensity in the ultraviolet area were improved through the ET. All the results indicated that $\text{LaInO}_3: \text{Bi}^{3+}:\text{Tb}^{3+}$ can be efficient green-emitting phosphors for field emission display device (FEDs) applications.

Acknowledgements

The authors are grateful to Chemistry Division, Bhabha Atomic Research Centre (BARC) for PL studies and Dr. R. David Kumar, Principal, Government College (A), Rajamahendravaram, Andhra Pradesh for necessary lab facilities.

References

- Jing Y. D, Zhang F., Summers C. J., and Wang Z. L., *Appl. Phys. Lett.*, 1999, 74, 1677
- Robert P, Seisenbaeva G. A, Wiglusz R. J, Kepinski L and Kessler V. G., *Inorg. Chem.* 2011, 50, 2966.
- Liu X and Lin J., *Solid State Sci.* 2009, 11, 2030.
- Lakshminarasimhan N and Varadaraju U.V., *Mater. Res. Bull.* 2006, 41, 724.
- He H, Huang X and Chen L., *Electrochimica acta*, 2001, 46, 2871-2877.
- Sood K, Singh K and Pandey O., *Transactions of the Indian Ceramic Society*, 2013, 72, 32-35.
- Chaluvadi S. K, Aswin V, Kumar P, Singh P, Haranath D, Rout P. K and Dogra A, *Journal of Luminescence*, 2015, 166, 244-247.
- Liu X, Yan L. and J. Lin., *Journal of The Electrochemical Society*, 2009, 156, P1-P6.
- Liu X. and Lin J., *Solid state sciences*, 2009, 11, 2030-2036.
- Shang Y, Yang P, Wang W, Wang Y, Niu N, Gai S. and Lin J., *Journal of Alloys and Compounds*, 2011, 509, 837-844.
- van Steensel L. I, Bokhove S. G, van de Craats A. M, de Blank J. and Blasse G., *Materials Research Bulletin*, 1995, 30, 1359-1362.
- Xu M, Wang L, Jia D, Le F., *J. Lumin.* 2015, 158, 125-129.
- Zhang Q, Ni H, Wang L, Xiao F., *Ceram. Int.* 2016, 42 (5), 6115-6120.
- Zhang W, Huang Y, Seo H.J., *Ceram. Int.* 2013, 39(4), 4313-4319.
- Blasse G, Grabmaier B.C., *Lumin. Mater.*, Springer press, Berlin, 1994, 91.

16. Samuel T, Satya Kamal Ch, Sujatha K, Veeraiah V, Ramakrishana Y, Ramachandra Rao K., *Optik* 2016, 127, 10575–10587.
17. Samuel T, Satya Kamal Ch, Ravipati S, Ajayi B. P, VeeraiahV, SudarsanV, Ramachandra Rao K., *Optical Materials* 2017, 69, 230-237
18. Satya Kamal Ch, Visweswara RaoT. K, ReddyP. V. S. S. N, SujathaK, AjayiB.P, JasinskiJ. B, Ramachandra RaoK., *RSC Adv.*,2017, 7, 9724
19. BoutinaudP., *Inorganic chemistry*, 2013, 52, 6028-6038.
20. WangL, LvZ, KangW, Shangguan X, Shi J. and HaoZ., *Applied Physics Letters*, 2013, 102, 151909.
21. WangL, SunQ, Liu Qand ShiJ., *Journal of Solid State Chemistry*, 2012, 191, 142-146.
22. JuH, Deng W, Wang B, Liu J, Tao Xand XuS., *Journal of alloys and compounds*, 2012, 516, 153-156.
23. S. R. R.G, BuddhuduS, *Mater. Lett.* 2008,62, 1259.
24. Hu C, Zhang Z, Liu H, Gao P, Wang Z. L., *Nanotechnology*, 2006,17, 5983.
25. L. Chen, K.J. Chen, S.F. Hu, R. S. LiuJ. *Mater. Chem*, 2011,21, 3677-3685.
26. H. He, R. Fu, Y. Cao, X. Song, Z. Pan, X. Zhao, Q. Xiao, R. Li, *Opt. Mater*, 2010, 32, 632-636.
27. G. Blasse, *Philips Res. Rep*, 1969,24131-144.
28. T. Miyakawa, D.L. Dexter, *Phys.Rev.B1*, 1970, 2961.
